Flattening and kinematics of the Galactic halo

Marel, R.P. van der

Mon. Not. R. astr. Soc. (1991) **248,** 515–522

Flattening and kinematics of the galactic halo

Roeland P. van der Marel
Sterrewacht Leiden, Postbus 9513, 2300 RA Leiden, The Netherlands

Accepted 1990 September 6. Received 1990 July 23

SUMMARY

The Jeans equations are used to study the galactic halo. Relations are derived between the axial ratio q of the metal-poor halo, the axial ratio $\tilde{q}$ of the dark halo, and the local velocity ellipsoid of metal-poor halo stars. Comparison with observational data implies that (i) neither models in which the principal axes of the velocity ellipsoid align with cylindrical coordinate axes, nor models in which they align with spherical coordinate axes can be ruled out by the presently available observational data; (ii) if the principal axes of the velocity ellipsoid align with cylindrical coordinate axes, then $q < 0.67$; (iii) if the metal-poor halo and the dark halo have the same axis ratio, then $q = \tilde{q} > 0.53$; (iv) the axial ratio of the dark halo must satisfy $\tilde{q} > 0.34$.

1 INTRODUCTION

Star count data indicate that the galactic metal-poor halo has axial ratio $0.6 \leq q \leq 0.8$ (Gilmore, Wyse & Kuijken 1989; Wyse 1990, private communication). The value $q = 0.8$ has been advocated by Bahcall & Soneira (e.g. Bahcall 1986). More recently Wyse & Gilmore (1989) have argued for $q = 0.6$. The density distribution, as traced by RR Lyrae stars and globular clusters, is found to be well described by a power law with exponent ~ 3.5 (Saha 1985; Zinn 1985). There is some evidence (Saha 1985) that the density falls off more steeply (logarithmic density gradient ~ 5) for $R \gtrsim 20$ kpc, but it is not clear if this effect is real.

Studies of the kinematics of metal-poor halo stars in the solar neighbourhood indicate that their velocity dispersion tensor is anisotropic, typical values for σ_R, σ_ϕ and σ_z being 140, 100 and 100 km s^{-1} (Sommer-Larsen & Zhen 1990; Morrison, Flynn & Freeman 1990; Freeman 1990, private communication). The rotation of the population is generally found to be small, typically $v_{\rm rot} \lesssim 40$ km s^{-1}. Studies of more distant fields towards the galactic poles do not show a significant rise of σ_z with z (e.g. Freeman 1987; Ratnatunga & Freeman 1989; Sommer-Larsen & Christensen 1989).

One way to model this kinematical behaviour is to choose a potential consistent with the observed (flat) rotation curve of our Galaxy, choose a plausible distribution function f for the metal-poor halo, and then evaluate the kinematics of the population from f. The results obviously depend on the particular choices one makes. Early studies (White 1985; Levison & Richstone 1986; Binney & May 1986) agreed that star count data and kinematical data were inconsistent. At that time it was believed that $\sigma_z \approx 65$ km s^{-1}, which led to very flat models with $0.3 \leq q \leq 0.5$. These values were much lower than the value $q = 0.8$ inferred from star count data. It has only recently been realized that the kinematical samples then available were contaminated by thick-disc stars and that σ_z for local metal-poor halo stars is probably as high as 100 km s^{-1}. It is then possible to construct nearly round models that *are* consistent with the kinematical data, as do Sommer-Larsen (1987; see also Sommer-Larsen & Christensen 1989) and Arnold (1990). These models might even be too round if the metal-poor halo is as flat as $q = 0.6$, as argued by Wyse & Gilmore (1989). Dejonghe & de Zeeuw (1988a) discussed the possibility of using the more realistic Stäckel potentials, rather than the logarithmic potentials adopted by most authors. Sommer-Larsen & Zhen (1990) try to recover f solely from observations of *local* metal-poor halo stars. Their resulting model consists of two components: a main, nearly spherical component comprising the large majority of the mass in the metal-poor halo, and a highly flattened component, comprising about 40 per cent of the density at the Sun.

A different approach (White 1989; Sommer-Larsen & Christensen 1989) is to use the tensor virial theorem to find a relation between q and the *global* velocity dispersion anisotropy of the metal-poor halo. The use of this relation is limited, however, since only the *local* shape of the velocity ellipsoid of metal-poor halo stars is known.

The tensor virial theorem is the global average of the Jeans equations, which themselves are averages over velocity space of the collisionless Boltzmann equation. In the present paper we compromise between the approaches mentioned above, and study the Jeans equations. Several interesting questions can be addressed in this way.

Motion in a spherical potential well requires the principal axes of the velocity ellipsoid to align with spherical coordinate axes (Eddington 1915). Dejonghe & de Zeeuw (1988a) showed that in more realistic potentials the velocity ellipsoid also aligns approximately with spherical coordinate axes at large distances, whereas in the scale-free models of

Richstone (1980), with a slightly flattened logarithmic potential, the velocity ellipsoid aligns approximately with cylindrical coordinate axes. Binney & Spergel (1983) argue from orbit integrations that the truth lies somewhere between. In this paper, consistency is demanded between the star count data and the kinematical data on the metal-poor halo, and then the Jeans equations are used to constrain the tilt of the velocity ellipsoid of metal-poor halo stars above the equatorial plane. Furthermore the reason why σ_z remains small towards the galactic poles is studied. This is surprising since towards the galactic poles one samples more and more of σ_r in σ_z.

Another interesting problem which can be studied using the Jeans equations is the flattening of the galactic dark halo. *N*-body calculations in Cold Dark Matter models lead to very flat dark haloes. Carlberg (1990, private communication) finds an average dark halo axial ratio $\tilde{q}=0.46$ (in fact his dark haloes generally turn out to be triaxial; see also Frenk *et al.* 1988). Sciama (1990) has argued for very flat dark haloes on theoretical grounds. In the galactic metal-poor halo (axial ratio q) there must be enough vertical pressure (i.e. σ_z) to resist the gravitational force of the galactic dark halo. The observed values of q and σ_z therefore put a lower limit on the possible axial ratio of the galactic dark halo, which can be determined using the Jeans equations. It is interesting to compare this lower limit with that expected from the considerations above.

Throughout this paper it is assumed, unless stated otherwise, that in the solar neighbourhood $(\sigma_R,\ \sigma_\phi,\ \sigma_z)=(140,\ 100,\ 100)$ km s^{-1} and $V_c=220$ km s^{-1}. Since $v_{\rm rot}$ is dynamically insignificant (Freeman 1987), its influence on $\overline{v_\phi^2}$ is neglected.

In Section 2 the basic assumptions that underlie the calculations in this paper are described. In Sections 3 and 4 the Jeans equations are employed to find relations between the shape of the velocity ellipsoid of metal-poor halo stars in the equatorial plane and the axial ratios of the metal-poor halo and the dark halo. These relations are compared with the observations, and the implications for the structure of the metal-poor halo and the dark halo are studied. In Section 5 the Jeans equations are used to study the limiting behaviour of σ_z at high latitudes. Section 6 summarizes the main conclusions. Appendix A discusses the forces which correspond to the dark halo potential adopted.

2 THE BASIC ASSUMPTIONS

In the following, $(R,\ \phi,\ z)$ are cylindrical coordinates and $(r,\ \phi,\ \theta)$ are spherical coordinates; $\theta=90°$ corresponds to the plane $z=0$.

2.1 The galactic dark halo

The rotation curve of our Galaxy is observed to be rather flat out to at least 20 kpc from the centre (e.g. Rohlfs *et al.* 1986). It is assumed that this rotation curve is due to a *dark halo*. In this paper, variables associated with the dark halo are denoted by a tilde (e.g. $\tilde{\rho}$). The potential is denoted simply by Φ. A simple spherical potential-density pair for the dark halo (e.g. White 1985; Sommer-Larsen 1987; White 1989) is that of the *singular isothermal sphere*

$$\tilde{\rho}(r)=\frac{\tilde{\sigma}^2}{2\pi G r^2},\ \Phi(r)=\tilde{\sigma}^2\ln r^2,\ V_c^2=2\tilde{\sigma}^2, \tag{1}$$

but it is more plausible to assume that the dark halo is oblate. To model this, one can substitute

$$\tilde{\omega}^2\equiv\tilde{q}^2R^2+z^2\ (\tilde{q}\leq 1) \tag{2}$$

for r^2 in the *potential* of the singular isothermal sphere (Richstone 1980; Levison & Richstone 1986). In this case the equidensity surfaces of $\tilde{\rho}$ have dimples at the poles. In the present paper $\tilde{\omega}^2$ is substituted for r^2 in the *density* of the singular isothermal sphere (as also in Sommer-Larsen & Christensen 1989); all equidensity surfaces of the dark halo are thus oblate, with axial ratio $\tilde{q}$. Appendix A discusses the potential Φ that is generated by this density distribution and the forces which correspond to it.

2.2 The galactic metal-poor halo

The mass density of the metal-poor halo is denoted by ρ. In this paper all equidensity surfaces of the metal-poor halo are assumed to be *concentric but not necessarily similar spheroids*. The axial ratio of a particular equidensity surface is denoted by q. For future use I define

$$\alpha\equiv\lim_{z/R\to\infty}-\left(\frac{z}{\rho}\frac{\partial\rho}{\partial z}\right)=\lim_{z/R\to\infty}-\left(\frac{\partial\log\rho}{\partial\log z}\right), \tag{3a}$$

$$\beta\equiv-\left(\frac{R}{\rho}\frac{\partial\rho}{\partial R}\right)_{(R_\odot,z=0)}=-\left(\frac{\partial\log\rho}{\partial\log R}\right)_{(R_\odot,z=0)}, \tag{3b}$$

where α is assumed finite. Observations typically indicate $\alpha\approx\beta\approx 3.5$ (Saha 1985; Zinn 1985). These values are used in the rest of the paper unless stated otherwise.

2.3 Hydrostatic equilibrium in the equatorial plane

Hydrostatic equilibrium for a stellar system is described by the Jeans equations. Assuming axisymmetry, there are two non-trivial Jeans equations and, for fixed ρ and Φ, four unknowns, namely the three velocity dispersion components and the tilt of the velocity ellipsoid in the (R,z)-plane. Numerous authors have tried to obtain analytical, formal or numerical solutions of the Jeans equations (e.g. Bacon, Simien & Monnet 1983; Bacon 1985; Fillmore 1986; Dejonghe & de Zeeuw 1988b; Evans & Lynden-Bell 1989). In this paper some simplifying assumptions are made and properties of the possible solutions are derived without actually solving the equations.

No attempt is made to solve for the tilt of the velocity ellipsoid. Instead two cases for the direction of the principal axes of the velocity ellipsoid are studied: (I) they always align with cylindrical coordinate axes, or (II) they always align with spherical coordinate axes. In the following, these cases are referred to as 'the case of cylindrical alignment' and 'the case of spherical alignment', or simply as case I and case II. The results for these two cases are compared with the observations to find which case fits the data best.

In case I, $\overline{v_i v_j}=0$ for all $i\neq j$; $i, j\in\{R, \phi, z\}$. In case II, $\overline{v_k v_l}=0$ for all $k\neq l$; $k, l\in\{r, \phi, \theta\}$. In case I it is most convenient to use the Jeans equations in cylindrical coordinates. From the axisymmetry of the problem and the assumption that the metal-poor halo is stationary, these are (e.g. Binney & Tremaine 1988)

$$\frac{\partial(\rho\overline{v_R^2})}{\partial R}+\rho\left(\frac{\overline{v_R^2}-\overline{v_\phi^2}}{R}+\frac{\partial\Phi}{\partial R}\right)=0, \tag{4a}$$

$$\frac{\partial(\rho\overline{v_z^2})}{\partial z}+\rho\frac{\partial\Phi}{\partial z}=0, \tag{4b}$$

the remaining two equations being trivial. For case II it is more convenient to use the Jeans equations in spherical coordinates (e.g. Bacon *et al.* 1983)

$$\frac{\partial(\rho\overline{v_r^2})}{\partial r}+\frac{\rho}{r}[2\overline{v_r^2}-(\overline{v_\theta^2}+\overline{v_\phi^2})]+\rho\frac{\partial\Phi}{\partial r}=0, \tag{5a}$$

$$\frac{\partial(\rho\overline{v_\theta^2})}{\partial\theta}+\rho[(\overline{v_\theta^2}-\overline{v_\phi^2})\cot\theta]+\rho\frac{\partial\Phi}{\partial\theta}=0, \tag{5b}$$

the remaining two equations again being trivial.

In the equatorial plane ($z=0$), which is where the solar neighbourhood is located, equations (4a) and (5a) contain the term

$$\frac{\partial(\rho\overline{v_R^2})}{\partial R}=\overline{v_R^2}\frac{\partial\rho}{\partial R}\left(1+\left.\frac{\partial\log\overline{v_R^2}}{\partial\log\rho}\right|_{z=0}\right). \tag{6}$$

In Baade's window at a projected galactocentric distance of 0.5 kpc, the line-of-sight velocity dispersion is 113 ± 11 km s^{-1} (Mould 1983). Assuming $\beta\approx3.5$, one can estimate very crudely

$$\left.\frac{\partial\log\overline{v_R^2}}{\partial\log\rho}\right|_{z=0}\approx\frac{2}{3.5}\frac{\log(140/113)}{\log(8.5/0.5)}=0.04. \tag{7}$$

Clearly the second term in equation (6) contributes little to the pressure that balances the gravitational force in equations (4a) and (5a). Indeed, if this term is neglected, equation (4a) yields

$$(\beta-1)\overline{v_R^2}+\overline{v_\phi^2}=V_c^2, \tag{8}$$

and equation (5a) yields

$$(\beta-2)\overline{v_R^2}+\overline{v_\phi^2}+\overline{v_\theta^2}=V_c^2. \tag{9}$$

By substituting the observed kinematical quantities one finds that equation (8) is satisfied for $\beta\approx3$, whereas equation (9) is satisfied for $\beta\approx3.5$. Both values for β fit the available star count data well (Saha 1985; Zinn 1985). This supports the argument that that the second term in equation (6) does not provide a major contribution to the pressure of the system.

Similarly, in the equatorial plane ($z=0$), equations (4b) and (5b) contain the term

$$\frac{\partial(\rho\overline{v_z^2})}{\partial z}=\overline{v_z^2}\frac{\partial\rho}{\partial z}\left(1+\left.\frac{\partial\log\overline{v_z^2}}{\partial\log\rho}\right|_{R=R_\odot}\right). \tag{10}$$

Observations show that σ_z does not change significantly with height above the equatorial plane (e.g. Freeman 1987; Ratnatunga & Freeman 1989). This indicates that also the second term in equation (10) does not provide a major contribution to the pressure of the system.

As a consequence of the above, one can assume that the *shape* of the velocity ellipsoid with respect to its principal axes does not vary (i.e. *constant anisotropy*), and still maintains *approximate hydrostatic equilibrium* in the solar neighbourhood. In the following

$$\overline{v_R^2}\equiv\frac{1}{\gamma_R}\overline{v_z^2},\ \overline{v_\phi^2}\equiv\frac{1}{\gamma_\phi}\overline{v_z^2},\ \overline{v_r^2}\equiv\frac{1}{\Gamma_r}\overline{v_\theta^2},\ \overline{v_\phi^2}\equiv\frac{1}{\Gamma_\phi}\overline{v_\theta^2}. \tag{11}$$

In the equatorial plane $\gamma_R=\Gamma_r$ and $\gamma_\phi=\Gamma_\phi$. In case I it is thus assumed that $(\partial\gamma_i/\partial R)=(\partial\gamma_i/\partial z)=0$ $(i\in\{R,\phi\})$, and in case II that $(\partial\Gamma_j/\partial r)=(\partial\Gamma_j/\partial\theta)=0$ $(j\in\{r,\phi\})$. Note that it is *not* assumed that the *size* of the velocity ellipsoid is constant. The principal axes of the velocity ellipsoid align both with cylindrical *and* with spherical coordinate axes if $\overline{v^2}_R=\overline{v_z^2}=\overline{v_r^2}=\overline{v_\theta^2}$ for certain r. Consequently case I and case II yield the same results if $\gamma_R=\Gamma_r=1$. This is the case for all r if $f=f(E,L_z)$. The argument which justifies the above assumption is strictly *local*. One cannot expect to be able to construct a constant anisotropy model that describes the kinematical properties of the whole metal-poor halo.

White (1989) and Sommer-Larsen & Christensen (1989) use the tensor virial theorem to find a relation between $\langle\overline{v_z^2}\rangle/\langle\overline{v_e^2}\rangle$ and the axial ratio of the metal-poor halo; here $v_e^2\equiv\frac{1}{2}(\overline{v_R^2}+\overline{v_\phi^2})$ and $\langle\cdot\rangle$ denotes the density-weighted average over the system. One might argue that our calculations should yield the same results since constant anisotropy is assumed. This is not so, for two reasons. First the tensor virial theorem treats $\overline{v^2}_R$ and $\overline{v_\phi^2}$ on an equal footing (which is certainly not justified by the observations), whereas we do not. Secondly, the relation that results from the tensor virial theorem has no clear interpretation if the velocity ellipsoid does not align with cylindrical coordinate axes everywhere.

3 THE JEANS EQUATIONS FOR CONSTANT ANISOTROPY SYSTEMS

In this section it is demonstrated that the assumption of constant anisotropy makes it possible to split the Jeans equations into one equation relating the *size* of the velocity ellipsoid to ρ and Φ, and one equation relating the *shape* of the velocity ellipsoid to ρ and Φ.

3.1 Case I: cylindrical alignment

First substitute equations (11) in equations (4). These are then two partial differential equations for $\overline{v_z^2}$. Equation (4a) yields

$$\frac{\partial\rho\overline{v_z^2}}{\partial R}=\left(\frac{\gamma_R}{\gamma_\phi}-1\right)\frac{\rho\overline{v_z^2}}{R}-\gamma_R\rho\frac{\partial\Phi}{\partial R}. \tag{12}$$

Then take the derivative of equation (4b) with respect to R, and substitute $(\partial^2/\partial z\,\partial R)$ for $(\partial^2/\partial R\,\partial z)$. Substitution of

equation (12) and subsequently of equation (4b) then yields

$$\left[-\frac{\rho}{R}\left(\frac{\gamma_R}{\gamma_\phi}-1\right)+\frac{\partial\rho}{\partial R}\right]\frac{\partial\Phi}{\partial z}-\left(\gamma_R\frac{\partial\rho}{\partial z}\right)\frac{\partial\Phi}{\partial R}$$

$$+[(1-\gamma_R)\rho]\frac{\partial^2\Phi}{\partial R\,\partial z}=0. \qquad (13)$$

3.2 Case II: spherical alignment

First substitute equations (11) in equations (5). These are then two partial differential equations for $\overline{v_\theta^2}$. Equation (5a) yields

$$\frac{\partial\rho\overline{v_\theta^2}}{\partial r}=\left(\Gamma_r+\frac{\Gamma_r}{\Gamma_\phi}-2\right)\frac{\rho\overline{v_\theta^2}}{r}-\Gamma_r\rho\frac{\partial\Phi}{\partial r}. \qquad (14)$$

Then take the derivative of equation (5b) with respect to r and substitute $(\partial^2/\partial\theta\,\partial r)$ for $(\partial^2/\partial r\,\partial\theta)$. Substitution of equation (14) and subsequently of equation (5b) then yields

$$\left[-\frac{\rho}{r}\left(\Gamma_r+\frac{\Gamma_r}{\Gamma_\phi}-2\right)+\frac{\partial\rho}{\partial r}\right]\frac{\partial\Phi}{\partial\theta}-\left[\rho\cot\theta\left(\Gamma_r-\frac{\Gamma_r}{\Gamma_\phi}\right)+\Gamma_r\frac{\partial\rho}{\partial\theta}\right]$$

$$\times\frac{\partial\Phi}{\partial r}+[(1-\Gamma_r)\rho]\frac{\partial^2\Phi}{\partial r\,\partial\theta}=0. \qquad (15)$$

3.3 Applications

The set of equations (12) and (13) or (14) and (15) can be used to construct constant anisotropy systems which are consistent with respect to the Jeans equations. One can, for example, substitute the spherical logarithmic potential (equation 1) into equation (15) and solve for ρ. This leads to the models of White (1985). However, as explained in Section 2.3, such models with constant anisotropy on a global scale are not of primary interest in the context of the galactic metal-poor halo (unless one builds a superposition of several such models, as does White 1985).

Instead, in the next section, *both* Φ and ρ (as defined in Sections 2.1 and 2.2) are specified in equation (13) or (15). The results then correspond to the *approximate* hydrostatic equilibrium described in Section 2.3.

4 THE VELOCITY ELLIPSOID IN THE EQUATORIAL PLANE

In this section, equation (13) (for the case of cylindrical alignment) and equation (15) (for the case of spherical alignment) are used to derive a relation between the shape of the velocity ellipsoid in the equatorial plane, the axial ratio q of the metal-poor halo, and the axial ratio $\tilde{q}$ of the dark halo. These relations are then compared with the observations.

4.1 Case I: cylindrical alignment

The potential Φ is assumed to be as in Section 2.1 and Appendix A. By using equations (A3) and (A8), $(\partial\Phi/\partial R)$ and $(\partial^2\Phi/\partial R\,\partial z)$ may be eliminated from equation (13), to yield

$$\frac{r^2}{2\tilde{\sigma}^2 z}\left(\frac{\partial\Phi}{\partial z}\right)=\frac{A}{B}, \qquad (16a)$$

where

$$A\equiv\gamma_R\frac{K(\tilde{q})}{2\tilde{q}}\frac{r^2}{z^2}\left(\frac{z}{\rho}\frac{\partial\rho}{\partial z}\right)+(1-\gamma_R)\frac{R^2}{\tilde{\omega}^2}, \qquad (16b)$$

$$B\equiv\left(1-\frac{\gamma_R}{\gamma_\phi}\right)+\left(\frac{R}{\rho}\frac{\partial\rho}{\partial R}\right)+\gamma_R\left(\frac{z}{\rho}\frac{\partial\rho}{\partial z}\right)+(\gamma_R-1)\frac{R^2}{r^2}. \qquad (16c)$$

The function $K(\tilde{q})$ is defined in equation (A4) and is related in a very simple way to the circular speed in the equatorial plane V_c^2 (equation A7). For comparison with kinematical data on metal-poor halo stars in the solar neighbourhood, we study the case $z\to 0$. For ρ as in Section 2.2,

$$\left(\frac{z}{\rho}\frac{\partial\rho}{\partial z}\right)=\frac{z^2}{q^2R^2}\left(\frac{R}{\rho}\frac{\partial\rho}{\partial R}\right)\qquad(z\to 0). \qquad (17)$$

We substitute equations (3) and (17) in equations (16b) and (16c) and then evaluate A and B for $z\to 0$. From equation (A2) it follows that the left-hand side of equation (16a) tends to $(1/\tilde{q}^2)$ for $z\to 0$. Rearranging terms, equation (16a) then yields

$$\frac{\tilde{q}K(\tilde{q})}{q^2}=\left(\frac{2}{\beta}\right)\left(-2+\frac{1}{\gamma_\phi}+\frac{\beta+1}{\gamma_R}\right)\qquad(z\to 0). \qquad (18)$$

4.2 Case II: spherical alignment

The potential Φ is assumed to be as in Section 2.1 and Appendix A. By using equations (A5) and (A6), $(\partial\Phi/\partial r)$ and $(\partial\Phi/\partial\theta)$ may be eliminated from equation (15), and setting $(\partial^2\Phi/\partial r\,\partial\theta)=0$ this yields

$$\frac{r^2}{2\tilde{\sigma}^2 z}\left(\frac{\partial\Phi}{\partial z}\right)=\frac{C}{D}, \qquad (19a)$$

where

$$C\equiv\frac{K(\tilde{q})}{2\tilde{q}}\left[-\Gamma_r\frac{R}{z}\left(\frac{1}{\rho}\frac{\partial\rho}{\partial\theta}\right)+\left(\frac{r}{\rho}\frac{\partial\rho}{\partial r}\right)+2(1-\Gamma_r)\right], \qquad (19b)$$

$$D\equiv 2-\Gamma_r-\frac{\Gamma_r}{\Gamma_\phi}+\left(\frac{r}{\rho}\frac{\partial\rho}{\partial r}\right). \qquad (19c)$$

The derivatives of ρ with respect to the coordinates r and θ can be expressed in terms of the derivatives of ρ with respect to R and z. For ρ as in Section 2.2, this yields for the solar neighbourhood ($R=R_\odot$ and $z\to 0$) (using equations 3 and 17)

$$\left(\frac{r}{\rho}\frac{\partial\rho}{\partial r}\right)=-\beta\left(1+\frac{z^2}{q^2R^2}\right),\ \left(\frac{1}{\rho}\frac{\partial\rho}{\partial\theta}\right)=-\beta\frac{z}{R}\left(1-\frac{1}{q^2}\right)\quad(z\to 0). \qquad (20)$$

Substitute equations (20) in equations (19b) and (19c) and then evaluate C and D for $z \to 0$. From equation (A2) it follows that the left-hand side of equation (19a) tends to $(1/\tilde{q}^2)$ for $z \to 0$. Rearranging terms, equation (19a) then yields

$$\frac{\tilde{q}K(\tilde{q})}{q^2} = \left(\frac{2}{\beta}\right)\left(1 + \frac{1}{\Gamma_\phi} + \frac{\beta-2}{\Gamma_r}\right) - \tilde{q}K(\tilde{q})\left(\frac{\beta-2}{\beta}\right)\left(\frac{1}{\Gamma_r} - 1\right) \qquad (z \to 0). \qquad (21)$$

This is the analogue of equation (18) for the case of spherical alignment.

4.3 Comparison with observations

Fig. 1 depicts the relation between q (the axial ratio of the metal-poor halo) and $\tilde{q}$ (the axial ratio of the dark halo) implied by equation (18) (for the case of cylindrical alignment of the velocity ellipsoid) and equation (21) (for the case of spherical alignment of the velocity ellipsoid). It follows directly that the metal-poor halo must be flatter than $q = 0.67$ if the velocity ellipsoid aligns with cylindrical coordinate axes.

Fig. 1 shows that spherical alignment of the velocity ellipsoid implies a more spherical metal-poor halo than cylindrical alignment (for the same value of $\tilde{q}$). This can be understood from equations (18) and (21). In the case of cylindrical alignment (equation 18), the axial ratio q correlates predominantly with the anisotropy $(\sigma_z/\sigma_R)_{z=0}$. In the case of spherical alignment (equation 21), the axial ratio q correlates predominantly with the anisotropy $(\sigma_z/\sigma_\phi)_{z=0}$ [note that Γ_r drops out of equation (21) for $\tilde{q} = 1$]. Since the former ratio is smaller than the latter, cylindrical alignment leads to a flatter metal-poor halo. This can also be argued more intuitively. In the solar neighbourhood the velocity dispersion parallel to the equatorial plane exceeds that perpendicular to it. Any tilting of the velocity ellipsoid therefore increases the vertical pressure (i.e. σ_z) away from the equatorial plane, leading to a more spherical metal-poor halo.

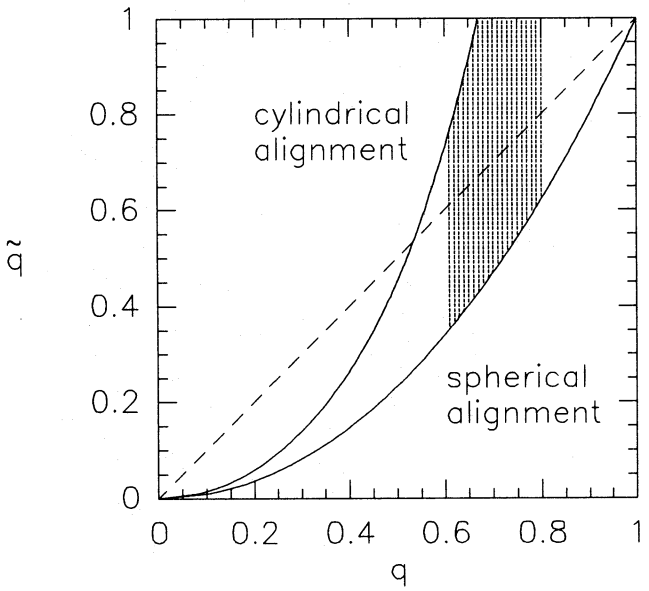

Figure 1. The solid lines show the relation between q (the axis ratio of the metal-poor halo) and $\tilde{q}$ (the axis ratio of the dark halo) as determined by equations (18) and (21). The shaded area is the region allowed by the observations ($0.6 \le q \le 0.8$). The dashed line is the line $q = \tilde{q}$. It is assumed that $(\sigma_R, \sigma_\phi, \sigma_z) = (140, 100, 100)$ km s^{-1} in the solar neighbourhood and that $\beta = 3.5$.

From the above argument it follows that models in which the velocity ellipsoid does tilt, but not as much as in the spherical alignment case, fall between the two curves in Fig. 1. This is therefore the region allowed by the kinematical data. Note, however, that not all models in this region are necessarily dynamically possible. In a spherical potential ($\tilde{q} = 1$) for example, the velocity ellipsoid *must* align with spherical coordinate axes (Eddington 1915).

The above results are consistent with other models. Sommer-Larsen (1987) and Arnold (1990) construct (nearly) spheroidal models for the metal-poor halo in which which the velocity ellipsoid aligns with spherical coordinate axes (Φ as in equation 1). Indeed they find that spherical models fit the data reasonably well. White (1989) shows from the tensor virial theorem that models in which the velocity ellipsoid is constant in cylindrical coordinates must be significantly flatter.

One could imagine models in which the shape of the metal-poor halo traces the shape of the dark halo (i.e. $q = \tilde{q}$). Fig. 1 shows that kinematical observations in the solar neighbourhood only allow such models if $q = \tilde{q} > 0.53$. Star count data indicate that the galactic metal-poor halo has axial ratio $0.6 \le q \le 0.8$ (Section 1). Taking this into account, the allowed region in Fig. 1 reduces to the shaded area. The observations put a lower limit on the flattening of the dark halo, as was explained in Section 1. Fig. 1 shows that this lower limit is $\tilde{q} > 0.34$ (corresponding to the lower left-hand corner of the shaded area).

Fig. 1 shows that neither cylindrical alignment models nor spherical alignment models are ruled out by the presently available data. The allowed cylindrical alignment models (the ones that border the shaded area in Fig. 1) have a dark halo which is much rounder than the metal-poor halo, whereas the allowed spherical alignment models have a dark halo which is much flatter than the metal-poor halo. The truth probably lies somewhere between, i.e. the velocity ellipsoid does tilt, but not as much as in the spherical alignment case. This is consistent with the conclusion that Binney & Spergel (1983) drew from orbit integrations.

5 σ_z AT HIGH LATITUDES

In this section the behaviour of σ_z at high latitudes ($z/R \to \infty$) is studied by using a slightly more general potential than in the previous sections. It is assumed to be of the form

$$\Phi = \Sigma^2[\ln r^2 + h(\theta)], \qquad (22)$$

where Σ [km s^{-1}] is a constant and $h(\theta)$ is any function for which $h'(\theta)$ is finite for all values of θ (such that the force on a test particle in this potential vanishes for $r \to \infty$). Note that the potential in Section 2.1 and Appendix A is of this form. The circular velocity in the equatorial plane is determined by $V_c^2 = 2\Sigma^2$.

In the following, $W \equiv \overline{v_z^2}/V_c^2$. Again, models are studied which have the property of constant anisotropy (Section 2.3). The cases of cylindrical alignment and of spherical alignment are studied separately, and the results are compared with the observations.

5.1 Case I: cylindrical alignment

From equation (4b) one directly obtains that

$$\frac{\partial W}{\partial z} = \frac{1}{z}(W\alpha - 1) \qquad (z/R \rightarrow \infty). \tag{23}$$

A physical solution for W must remain finite for $z/R \rightarrow \infty$. From equation (23) it follows that there is always one such solution, for which at fixed R

$$\lim_{z\rightarrow\infty} W(z) = \frac{1}{\alpha}. \tag{24}$$

5.2 Case II: spherical alignment

One wants to use the Jeans equations in cylindrical coordinates to find for every fixed R an ordinary differential equation for $\overline{v_z^2}$ as function of z. However, equations (4) cannot be used since in general the mixed second-order moment $\overline{v_R v_z}$ does not vanish if the velocity ellipsoid aligns with spherical coordinate axes. Instead the slightly more complicated equations (Binney & Tremaine 1988)

$$\frac{\partial \rho \overline{v_R^2}}{\partial R} + \frac{\partial \rho \overline{v_R v_z}}{\partial z} + \rho\left(\frac{\overline{v_R^2} - \overline{v_\phi^2}}{R} + \frac{\partial \Phi}{\partial R}\right) = 0, \tag{25a}$$

$$\frac{\partial \rho \overline{v_z^2}}{\partial z} + \frac{\partial \rho \overline{v_R v_z}}{\partial R} + \rho\left(\frac{\overline{v_R v_z}}{R} + \frac{\partial \Phi}{\partial z}\right) = 0, \tag{25b}$$

must be used. By definition $v_z = v_r \cos\theta - v_\theta \sin\theta$ and $v_R = v_r \sin\theta + v_\theta \cos\theta$. Since $\overline{v_r v_\theta} = 0$ in case II,

$$\overline{v_R^2} = \frac{1 + [(1/\Gamma_r) - 1]\sin^2\theta}{1 + [(1/\Gamma_r) - 1]\cos^2\theta}\,\overline{v_z^2}, \tag{26}$$

with similar expressions for $\overline{v_R v_z}$ and $\overline{v_\phi^2}$. These equations are substituted in equations (25) to obtain two partial differential equations for $\overline{v_z^2}$. Elimination of $(\partial \overline{v_z^2}/\partial R)$ from these equations yields for every fixed R an ordinary differential equation for $\overline{v_z^2}$ as function of z. It can be shown that for $z/R \rightarrow \infty$ this equation is

$$\frac{\partial W}{\partial z} = \frac{1}{z}\left\{W\left[\alpha + (\Gamma_r - 1)\left(1 + \frac{1}{\Gamma_\phi}\right)\right] - 1\right\} \qquad (z/R \rightarrow \infty). \tag{27}$$

A physical solution for W must remain finite for $z/R \rightarrow \infty$. From equation (27) it follows that there is always one such solution, for which at fixed R

$$\lim_{z\rightarrow\infty} W(z) = \lim_{z\rightarrow\infty} \frac{1}{\alpha + (\Gamma_r - 1)[1 + (1/\Gamma_\phi)]}. \tag{28}$$

5.3 Comparison with observations

Equation (24) for case I yields $\sigma_z \approx V_c/\sqrt{\alpha}$ at high latitudes, i.e. 118 km s^{-1} for $\alpha = 3.5$ and 98 km s^{-1} for $\alpha = 5$ (Saha 1985). Even in the latter case, σ_z is still higher than the observed value (e.g. Freeman 1987; Sommer-Larsen & Christensen 1989). This seems to rule out the suggestion of Freeman (1987) that the velocity dispersions are constant in cylindrical coordinates.

From equation (28) for case II it follows that the value of σ_z at high latitudes depends on the shape of the velocity ellipsoid at high latitudes. If $\overline{v_\theta^2} < \overline{v_r^2}$ for $z/R \rightarrow \infty$, then $\sigma_z > V_c/\sqrt{\alpha}$. Again this is too high to be consistent with observational data. If, however, $\overline{v_\theta^2} > \overline{v_r^2}$ for $z/R \rightarrow \infty$, then σ_z is much closer to the observed value.

The low observed value of σ_z at high latitudes thus favours models in which the velocity ellipsoid aligns (approximately) with spherical coordinate axes and which have $\overline{v_\theta^2} > \overline{v_r^2}$ at high latitudes. Indeed, the models of White (1985), Sommer-Larsen (1987) and Dejonghe & de Zeeuw (1988a), which were constructed to fit the kinematical data on the metal-poor halo all have these properties. Sommer-Larsen & Christensen (1989) discussed qualitatively a model for the formation of the galactic halo in which such a situation could arise. In any model in which the velocity ellipsoid aligns with spherical coordinate axes, $v_R^2 = v_z^2$ at $\theta = 45°$. Since the above indicates that $v_R^2 > v_z^2$ at high latitudes, it might be expected that towards the galactic poles σ_z takes on a maximum value at a height of ~ 10 kpc above the galactic plane. Interestingly, this is consistent with the observations by Sommer-Larsen & Christensen (1989).

6 CONCLUSIONS

In this paper, assumptions are made about the potential of the dark halo (Section 2.1), about the mass density of the metal-poor halo (Section 2.2), and about the tilt and shape of the velocity ellipsoid (Section 2.3). The Jeans equations are used to find relations between q (the axial ratio of the metal-poor halo), $\tilde{q}$ (the axial ratio of the dark halo) and the shape of the velocity ellipsoid. These relations are compared with the observations.

From the local shape of the velocity ellipsoid of metal-poor halo stars $[(\sigma_R, \sigma_\varphi, \sigma_z) = (140, 100, 100)$ km s$^{-1}]$ it can be derived that:

(i) if the principal axes of the velocity ellipsoid align with spherical coordinate axes, then the metal-poor halo must be significantly more spherical than when the principal axes align with cylindrical coordinate axes;

(ii) if the principal axes of the velocity ellipsoid align with cylindrical coordinate axes, then $q < 0.67$;

(iii) if the metal-poor halo and the dark halo have the same axial ratio, then $q = \tilde{q} > 0.53$.

If one furthermore uses the constraint $0.6 \leq q \leq 0.8$, as indicated by star count data, then:

(iv) the axial ratio of the dark halo must satisfy $\tilde{q} > 0.34$;

(v) neither models in which the principal axes of the velocity ellipsoid align with cylindrical coordinate axes, nor models in which they align with spherical coordinate axes can be ruled out by the presently available observational data. The truth most likely lies somewhere between.

A study of the behaviour of σ_z for $z/R \to \infty$ for solutions of the Jeans equations shows that:

(vi) the observation that σ_z remains small towards the galactic poles favours models in which the principal axes of the velocity ellipsoid align approximately with spherical coordinate axes, and $\overline{v_\theta^2} > \overline{v_r^2}$ at high latitudes. An increase in the logarithmic density gradient with increasing galactocentric distance (e.g. Saha 1985) would also help to keep σ_z small at high latitudes.

ACKNOWLEDGMENTS

The author thanks Tim de Zeeuw for many helpful discussions and for being a very stimulating advisor, also Bernard Jones, Ken Freeman, Vincent Icke and Herwig Dejonghe for reading an early version of the manuscript and providing useful comments. Stimulating discussions with Rosemary Wyse and Ray Carlberg are acknowledged. The author thanks the Leids Kerkhoven-Bosscha Fonds and the Aspen Center for Physics for providing grants and for the opportunity to work on this project in a stimulating atmosphere in Aspen, Colorado.

REFERENCES

Arnold, R., 1990. *Mon. Not. R. astr. Soc.*, **244,** 465.
Bacon, R., 1985. *Astr. Astrophys.*, **143,** 84.
Bacon, R., Simien, F. & Monnet, G., 1983. *Astr. Astrophys.*, **128,** 405.
Bahcall, J. N., 1986. *Ann. Rev. Astr. Astrophys.*, **24,** 577.
Binney, J. J. & Spergel, D. N., 1983. In: *The Nearby Stars and the Stellar Luminosity Function, IAU Colloq. No. 76,* eds Philip, A. G. D. & Upgren, A. R., p. 259. Davis Press, Schenectady, N.Y.
Binney, J. J. & May, A., 1986. *Mon. Not. R. astr. Soc.*, **218,** 743.
Binney, J. J. & Tremaine, S., 1988. *Galactic Dynamics*, Princeton University Press.
Dejonghe, H. & de Zeeuw, P. T., 1988a. *Astrophys. J.*, **329,** 720.
Dejonghe, H. & de Zeeuw, P. T., 1988b. *Astrophys. J.*, **333,** 90.
de Zeeuw, P. T. & Pfenniger, D., 1988. *Mon. Not. R. astr. Soc.*, **235,** 949.
Eddington, A. S., 1915. *Mon. Not. R. astr. Soc.*, **76,** 37.
Evans, N. W. & Lynden-Bell, D., 1989. *Mon. Not. R. astr. Soc.*, **236,** 801.
Fillmore, J. A., 1986. *Astr. J.*, **91,** 1097.
Freeman, K. C., 1987. *Ann. Rev. Astr. Astrophys.*, **25,** 603.
Frenk, C. S., White, S. D. M., Davis, M. & Efstathiou, G., 1985. *Astrophys. J.*, **327,** 507.
Gilmore, G., Wyse, R. F. G. & Kuijken, K., 1989. *Ann. Rev. Astr. Astrophys.*, **27,** 555.
Gradshteyn, I. S. & Ryzhik, I. M., 1965. *Table of Integrals, Series and Products,* Academic Press, San Diego.
Levison, H. F. & Richstone, D. O., 1986. *Astrophys. J.*, **308,** 627.
Morrison, H. L., Flynn, C. & Freeman, K., 1990. *Astr. J.*, **100,** 1191.
Mould, J., 1983. *Astrophys. J.*, **266,** 255.
Perek, L., 1962. *Adv. Astr. Astrophys.*, **1,** 165.
Ratnatunga, K. U. & Freeman, K. C., 1989. *Astrophys. J.*, **339,** 126.
Richstone, D. O., 1980. *Astrophys. J.*, **238,** 103.
Roberts, P. H., 1962. *Astrophys. J.*, **136,** 1108.
Rohlfs, K., Chini, R., Wink, J. E. & Böhme, R., 1986. *Astr. Astrophys.*, **158,** 181.
Saha, A., 1985. *Astrophys. J.*, **289,** 310.
Sciama, D. W., 1990.*Mon. Not. R. astr. Soc.*, **244,** 1P.
Sommer-Larsen, J., 1987. *Mon. Not. R. astr. Soc.*, **227,** 21P.
Sommer-Larsen, J. & Christensen, P. R., 1989. *Mon. Not. R. astr. Soc.*, **239,** 441.
Sommer-Larsen, J. & Zhen, C., 1990. *Mon. Not. R. astr. Soc.*, **242,** 10.
White, S. D. M., 1985. *Astrophys. J.*, **294,** L99.
White, S. D. M., 1989. *Mon. Not. R. astr. Soc.*, **237,** 51P.
Wyse, R. F. G. & Gilmore, G., 1989. *Comments Astrophys.*, **13,** 135.
Zinn, R., 1985. *Astrophys. J.*, **293,** 424.

APPENDIX A: THE POTENTIAL Φ OF THE DARK HALO

It is assumed that the mass density of the dark halo is $\tilde{\rho} = C\tilde{\omega}^{-2}$, where $C \equiv \tilde{\sigma}^2/2\pi G$ and $\tilde{\omega}^2$ is defined in equation (2). From the theory of Roberts (1962) (see also Binney & Tremaine 1988, page 57), it follows that

$$\Phi(R,z) = \frac{\tilde{\sigma}^2}{2\tilde{q}} \int_0^\infty \ln[R^2(\tilde{q}^2+\xi) + z^2(1+\xi)] \frac{d\xi}{(1+\xi)\sqrt{\tilde{q}^2+\xi}}. \tag{A1}$$

This integral cannot be expressed in terms of elementary functions. In the following, $\tilde{e}^2 \equiv |1-\tilde{q}^2|$. The forces in cylindrical coordinates are [use equations (2.225.1) and (2.246) from Gradshteyn & Ryzhik (1965)]

$$\frac{\partial\Phi}{\partial z} = \begin{cases} (2\tilde{\sigma}^2/r\tilde{q}\tilde{e})\arctan(z\tilde{e}/r\tilde{q}), & \text{if } \tilde{q}<1, \\ (2\tilde{\sigma}^2)(z/r^2), & \text{if } \tilde{q}=1, \\ (\tilde{\sigma}^2/r\tilde{q}\tilde{e})\ln[(r\tilde{q}+z\tilde{e})/(r\tilde{q}-z\tilde{e})], & \text{if } \tilde{q}>1, \end{cases} \tag{A2}$$

$$\frac{\partial\Phi}{\partial R} = (2\tilde{\sigma}^2/2R\tilde{q})\,K(\tilde{q}) - (z/R)\frac{\partial\Phi}{\partial z}. \tag{A3}$$

The function K is defined as

$$K(\tilde{q}) \equiv \int_0^\infty \frac{d\xi}{(1+\xi)\sqrt{\tilde{q}^2+\xi}} = \begin{cases} (2/\tilde{e})\arctan(\tilde{e}/\tilde{q}), & \text{if } \tilde{q}<1, \\ 2, & \text{if } \tilde{q}=1. \\ (1/\tilde{e})\ln[1+(\tilde{e}/\tilde{q})/1-(\tilde{e}/\tilde{q})], & \text{if } \tilde{q}>1. \end{cases} \tag{A4}$$

The forces in spherical coordinates follow from

$$\frac{\partial\Phi}{\partial r} = \frac{\tilde{\sigma}^2 K(\tilde{q})}{r\tilde{q}}, \tag{A5}$$

$$\frac{\partial\Phi}{\partial\theta} = \frac{z}{R}\frac{\tilde{\sigma}^2 K(\tilde{q})}{\tilde{q}} - \frac{r^2}{R}\frac{\partial\Phi}{\partial z}. \tag{A6}$$

The circular speed in the equatorial plane is

$$V_c^2(\tilde{q}) \equiv v_c^2(z=0) = R\left(\frac{\partial\Phi}{\partial R}\right)_{z=0} = \tilde{\sigma}^2\frac{K(\tilde{q})}{\tilde{q}}. \tag{A7}$$

Several of these formulae were already derived by Perek (1962), de Zeeuw & Pfenniger (1988) and Sommer-Larsen & Christensen (1989).

In this paper, expressions are also required for the second-order mixed derivatives of Φ. It follows from equation (A5) that $(\partial^2\Phi/\partial r\,\partial\theta)=(\partial^2\Phi/\partial\theta\,\partial r)=0$. Using equation (2.225.2) from Gradshteyn & Ryzhik (1965) it follows from equation (A1) that

$$\frac{\partial^2\Phi}{\partial z\,\partial R}=\frac{\partial^2\Phi}{\partial R\,\partial z}=(-2\tilde{\sigma}^2 zR/r^2\tilde{\omega}^2)-(R/r^2)\frac{\partial\Phi}{\partial z}. \qquad \text{(A8)}$$